

基于柔性超材料的高灵敏度拉力传感器

邓光晟^{1,2*}, 方林颖², 郭澳然², 杨军^{1,2}, 李迎^{1,2}, 尹治平^{1,2}¹合肥工业大学光电技术研究院特种显示与成像技术安徽省技术创新中心, 安徽 合肥 230009;²合肥工业大学仪器科学与光电工程学院测量理论与精密仪器安徽省重点实验室, 安徽 合肥 230009

摘要 提出了一种基于柔性超材料的高灵敏度拉力传感器,该超材料传感器由刻蚀在聚二甲基硅氧烷(PDMS)薄膜表面的多方形谐振单元的平面阵列组成。拉伸柔性PDMS薄膜会改变谐振单元的结构参数,进而使传感器的谐振频率产生变化。该超材料传感器可以同时实现应变或拉力的高灵敏度检测。同时,谐振结构中央的方形连接环起到了不对称分裂间隙的作用,激发了具有更高Q值的高阶谐振模式,实现了更高的频谱分辨率。实验结果表明,施加拉力从0增大至1.2 N时,结构尺寸拉伸率达到初始状态的1.2倍,超材料的谐振峰频率从109.23 GHz红移到99.42 GHz。该传感器可以实现8.43 GHz/N的高灵敏度拉力传感。耐久性测试表明在该样品的使用中至少可以经历100次拉伸-松弛循环。所提出的传感器具有灵敏度高、加工方便、成本低和无线测量的优点,具有潜在的应用价值。

关键词 传感器; 拉力传感器; 柔性; 超材料; 光谱; 高灵敏度

中图分类号 O436

文献标志码 A

DOI: 10.3788/AOS231287

1 引言

随着新兴材料的创新,柔性材料受到了极大的关注。柔性电子器件的独特优势,如超薄、可弯曲和质量轻,为开发下一代人体运动检测、健康监测和可穿戴设备铺平了道路^[1-3]。柔性拉力传感器作为外部机械信号的直接捕捉工具,是柔性传感系统中的重要组成部分^[4-5];同时,鉴于其在从电子皮肤到实时医疗健康监测等应用方面的巨大潜力,开发灵活、高拉伸率和高灵敏度的拉力传感器愈加迫切^[6-7]。柔性拉力传感器通常由敏感材料和基底组成,其性能受敏感材料和基底材料结构的影响很大。将柔性可拉伸聚合物与导电纳米材料相结合的方案在提高传感器的灵敏度和可拉伸性方面已经取得了一些进展,但实现高灵敏度和高精度检测仍然是目前亟须解决的柔性材料与传感器相结合方面的难题^[8],而柔性材料与超材料传感器的结合为解决上述难题提供了一种可行的方案^[9-10]。

近年来,超材料已日益成为电磁领域的研究热点之一^[11-14]。作为一种人工结构,超材料的电磁响应可以通过改变超材料的结构尺寸参数来灵活控制,这一特性为超材料在传感场合中的应用提供了基础。同时,超材料还可以增强光与物质的相互作用,进而显著提高器件的传感性能。通过引入如聚二甲基硅氧烷

(PDMS)、聚丙烯(PP)、聚对苯二甲酸乙二醇酯(PET)和聚萘二甲酸乙二醇酯(PEN)等柔性基底,可以构建柔性超材料^[15]。超材料传感器具有质量轻、成本低、便携等优点,日益吸引了各国研究人员的广泛关注。Pryce等^[16]使用PDMS衬底的大应变机械变形来控制传感器谐振元件之间的距离,并最终实现了谐振频率调谐。Zheng等^[17]在PEN衬底上制备了两种分别具有不对称和对称配置的柔性超材料,通过不同应力下的材料弯曲提供了连续的可调谐性。Li等^[18]提出了机械可调谐平面超材料,使用高弹性基底上的谐振元件实现了在小应变下谐振频率的连续可调谐。Jeong等^[19]提出了一种堆叠在印刷基板上的喷墨印刷导电图案,以实现吸收频率随接地层厚度变化的电磁压力传感器。上述超材料传感器虽然能够利用频谱分析的方法实现微小应力和应变的传感,但灵敏度和分辨率还相当有限。为了进一步提高超材料传感器的传感性能,迫切需要设计一种具有高品质因数和高灵敏度的超材料应力传感器。

本文在柔性基底上实现了超材料传感器,其谐振频率可以通过机械拉伸基底进行调谐。该超材料传感器由沉积在PDMS薄膜上的多方形谐振单元的平面阵列组成。设计的超材料传感器的谐振频率对方形贴片结构尺寸的变化非常敏感。实验结果表明,对于外

收稿日期: 2023-07-20; 修回日期: 2023-08-30; 录用日期: 2023-09-19; 网络首发日期: 2023-09-29

基金项目: 国家自然科学基金(62001150, 61871171)、安徽省自然科学基金(2208085MF160)、中央高校基本科研业务费资助(JZ2022HG TB0270)

通信作者: *dgsh@hfut.edu.cn

部施加的拉力,该传感器可以实现 8.43 GHz/N 的高灵敏度检测。此外,进一步通过拉伸-松弛循环实验验证了所提出结构具有良好的稳定性和耐久性。

2 设计与原理

本文所提出的超材料传感器的单元结构如图 1(a)所示。该结构由多个方形交叉金属谐振结构、PDMS 薄膜基底和涂覆在 PDMS 薄膜底部的金属层组成。金属层由铜制成,电导率为 5.88×10^7 S/m,而 PDMS 衬底的相对介电常数为 2.7,损耗角正切为 0.04。图 1(b)给出的谐振单元结构尺寸为:结构单元的初始周期长度 $L=4.0$ mm, $b_1=1.6$ mm, $b_2=1.0$ mm, $d_1=0.3$ mm, $d_2=0.4$ mm。此外,综合考虑所提出的柔性传感器的拉伸性和耐久性,PDMS 膜的

厚度 h 选择为 0.3 mm。使用有限元方法(FEM)模拟了所提出的传感器的反射系数 S_{11} 。考虑到电磁波由 z 方向入射,因此将 x 和 y 方向设置为周期边界条件,而 z 方向设定为开放边界条件。

模拟时,电场方向平行于 x 轴的平面电磁波入射到超材料的表面。传感器的吸收率可由反射系数推导得到:

$$A(\omega) = 1 - \Gamma(\omega) = 1 - |S_{11}(\omega)|^2, \quad (1)$$

式中: $\Gamma(\omega)$ 是随频率变化的反射率,其值等于反射系数 S_{11} 的平方。图 1(c)给出了模拟得到的反射系数和对应的吸收率。可以看出,谐振峰的频率为 108.88 GHz,吸收率达到 99.8%。这种强电磁共振显著提高了传感器的分辨率。

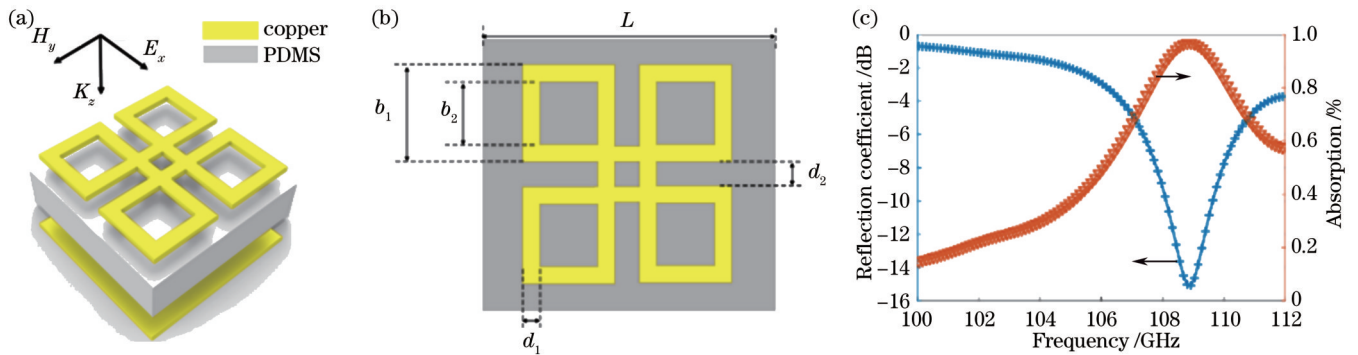


图 1 超材料传感器示意图及其频谱响应特性。(a)超材料传感器的单周期结构图;(b)谐振单元结构;(c)模拟得到的反射系数和吸收频谱

Fig. 1 Schematic diagram of metamaterial sensor and spectral response. (a) Single period structure diagram of metamaterial sensor; (b) resonance unit cell; (c) simulated reflection coefficient and absorption spectrum

为了研究该超材料传感器的谐振机制,模拟了金属谐振单元上表面电流的分布,结果如图 2 所示。对于本文提出的方形交叉谐振结构[图 2(a)],图 2(b)所示的表面电流分布表明其谐振模式中存在高阶偶极子共振。同时,对于如图 2(c)所示的没有中央方形连接环的谐振结构,表面电流流向与入射电磁波的电场方向平行[图 2(d)],仅有偶极子模式被激发。因此,尽管所提出的谐振单元结构为对称结构,但中央的方形连接环起到了不对称分裂间隙的作用^[20],进而产生具有更高 Q 值的电磁谐振,实现了更高的频谱分辨率。

由于 PDMS 介质基底为柔性材料,通过拉伸所得到的传感器,沿拉伸方向的结构尺寸将按比例增大,从而导致峰值谐振频率发生变化。结构尺寸拉伸率定义为 $\epsilon = \Delta L / L$,其中 ΔL 是拉伸后增大的尺寸。图 2(e)所示为当 L 由于拉伸而逐渐增大时谐振频率随拉伸率的变化情况。可以看到,当拉伸率从 0 增加到 20% 时,谐振峰频率从 108.88 GHz 红移到了 99.08 GHz。这里,用灵敏度 S 来衡量该传感器的传感性能,其定义为

$$S = \frac{\Delta f}{\epsilon}, \quad (2)$$

式中: Δf 是谐振频率的变化量。通过线性拟合数据计算得到的该超材料传感器的灵敏度在单位拉伸率下的频移可达到 48.04 GHz。需要指出的是,由于本传感器工作于低频太赫兹波段(约 0.1 THz),该灵敏度足以分辨由拉伸所导致的结构尺寸的微小变化。同时,对比分析了独立方环结构的反射频谱随拉伸率的变化情况,如图 2(f)所示。可以看出,当拉伸率较低时,该结构的谐振强度较弱,频率分辨率很低。

在谐振机理研究的基础上,进一步分析了传感器的结构参数变化对灵敏度的影响。如图 3(a)所示,环宽 d_1 的变化对谐振频率和 Q 值的影响较小。此外,从图 3(b)可以看出,当 d_1 的值为 0.3 mm 时,可以获得最高的传感灵敏度。图 3(c)给出了谐振频率随方环之间的距离 d_2 的变化情况。当 d_2 从 0.2 mm 增大到 0.5 mm 时,谐振频率向高频位置移动,而谐振强度随着 d_2 的增大而降低。此外,图 3(d)表明:当 d_2 为 0.4 mm 时,可以实现最佳的传感灵敏度,且此时传感器仍有较高的频率分辨率。PDMS 基底厚度对超材料传感器的谐振频率和灵敏度的影响如图 3(e)、(f)所示。通过减小 PDMS 层的厚度,可以获得更高的频率分辨率和更高的灵敏度;但

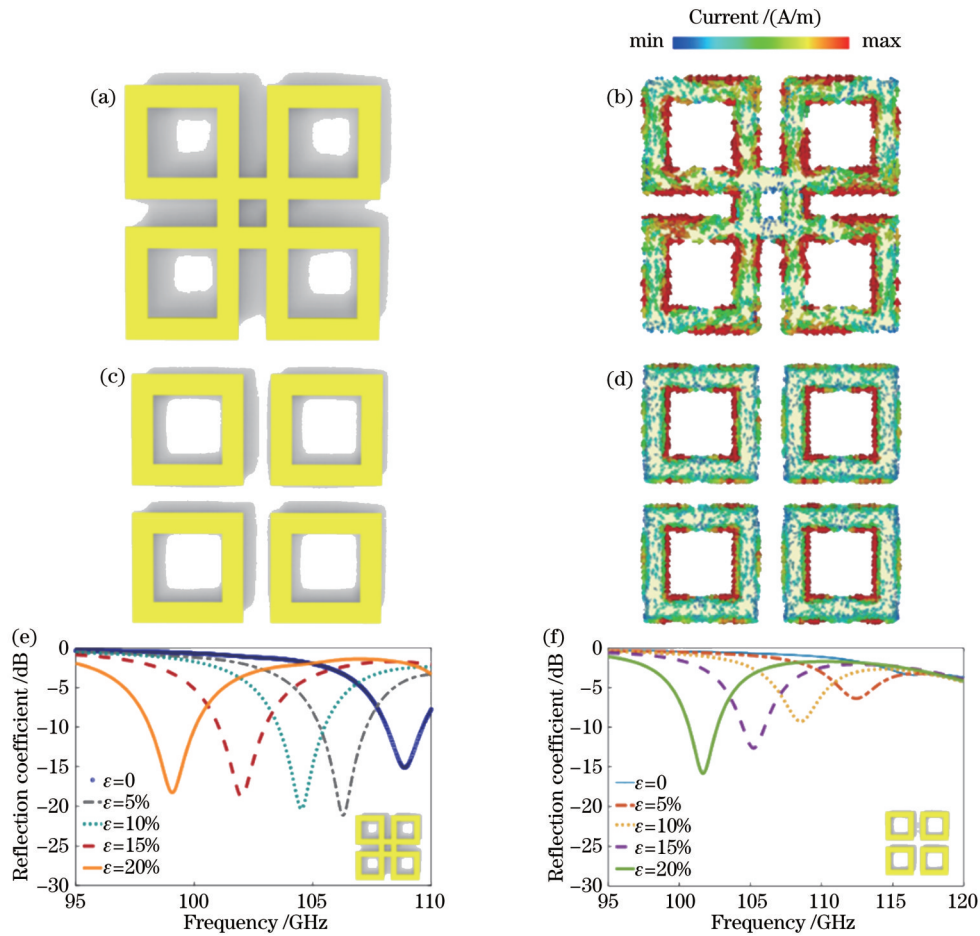


图 2 不同谐振单元的表面电流分布和响应频谱特性。(a)方形交叉谐振结构;(b)方形交叉谐振结构的表面电流分布;(c)独立方环结构;(d)独立方环结构的表面电流分布;(e)方形交叉谐振结构和(f)独立方环结构中反射系数与拉伸率ε的关系

Fig. 2 Surface current distributions and response spectra of different resonance unit cell. (a) Interconnected square resonance structure; (b) surface current distribution of interconnected square resonance structure; (c) split square ring structure; (d) surface current distribution of split square ring structure; dependence of reflection coefficient on elongated periodicity ϵ for (e) interconnected square resonance structure and (f) split square ring structure

过小的PDMS基底厚度会缩短器件的使用寿命。因此,最终选择了0.3 mm的PDMS基底厚度,以取得灵敏度和耐久性之间的平衡。表1给出了本文提出的传感器与一些已有报道的应变传感器的对比。对于传统的应变传感器,需要将物理变形转化为可测量的电信号输

出,因此普遍需要一个连接线来检测相应的电容或电阻变化。然而,本文提出的设计方案适用于无线连接以及非接触测量的场景(如精密工作台上加工工件的受力误差检测),传感器通过受力产生的形变带来的频谱实时变化显示误差,以便及时进行校正。

表 1 几种不同的应变传感器对比
Table 1 Comparison of several strain sensors

Ref. No	Sensitive material	Base material	Connectivity	Operation mode	Testing range / %	Accuracy / %
[21]	Graphene	PDMS	Wired	Capacitive change	7	11.8
[22]	Carbon nanotubes	PDMS	Wired	Resistive change	50	10.5
[23]	Silver nanowire	PDMS	Wired	Resistive change	70	—
[24]	Alginate-polyacrylamide hydrogel	Carbon black	Wired	Capacitive change	120	—
This paper	Metamaterial	PDMS	Wireless	Electromagnetism	20	5.9

3 实验与讨论

加工制备了所提出的超材料传感器样品并进行了

相关测试。首先,使用高温气相沉积法在0.3 mm厚的PDMS基底的两侧各蒸镀了一层500 nm厚的薄铜层。然后,通过湿法蚀刻,在PDMS基底的上表面光

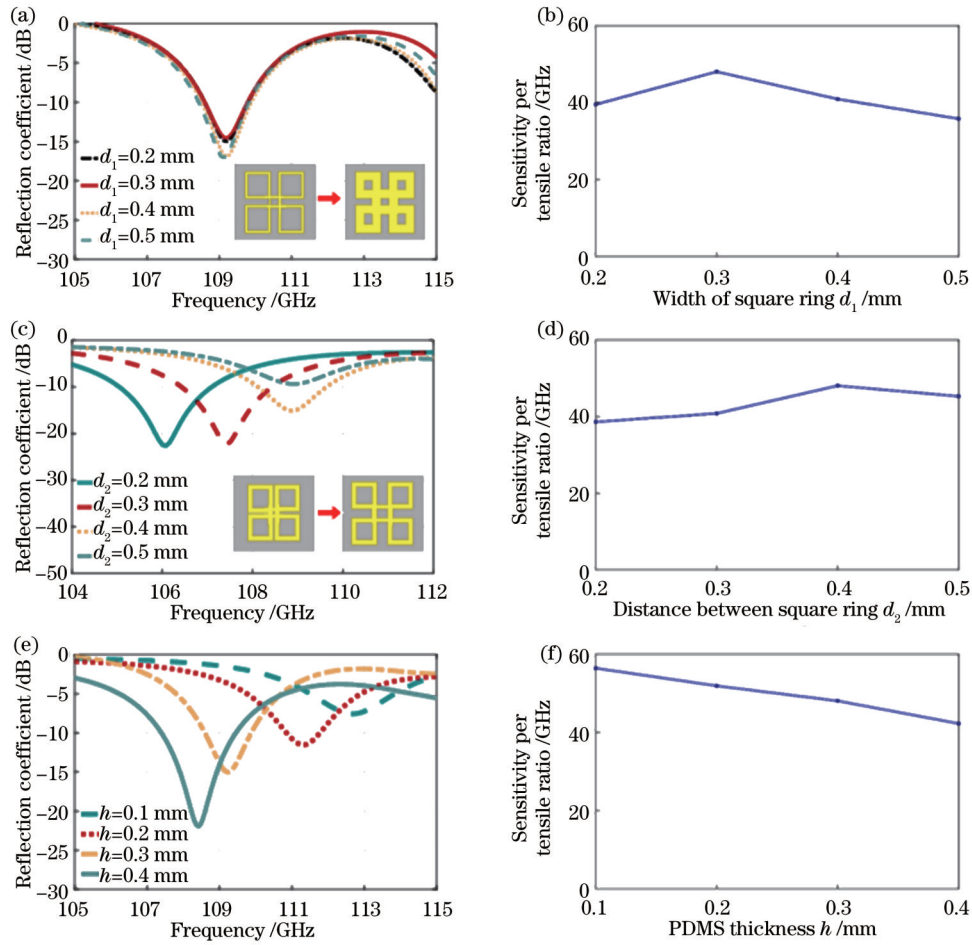


图 3 不同结构参数对反射系数和灵敏度的影响。(a)(b)方环宽度 d_1 的影响；(c)(d)方环之间的距离 d_2 的影响；(e)(f)PDMS 基底厚度 h 的影响

Fig. 3 Effects of different structural parameters on reflection coefficient and sensitivity. (a)(b) Effect of width of square ring d_1 ; (c)(d) effect of distance between square rings d_2 ; (e)(f) effect of PDMS substrate thickness h

刻出对应的谐振结构图案。图 4(a)为加工得到的样品照片，样品包含了 4×10 个单元阵列，尺寸为 $16 \text{ mm} \times 40 \text{ mm}$ 。测试采用的实验平台如图 4(b)所示，采用了矢量网络分析仪 (Agilent N5224A)、扩频模

块 (VDI VNAX600) 和工作在 F 频段 ($90 \sim 140 \text{ GHz}$) 的喇叭天线来测试不同拉伸状态下样品的反射频谱响应。此外，为了提高测试精度，采用了电子拉伸器精确控制施加在样品上的拉伸应力。

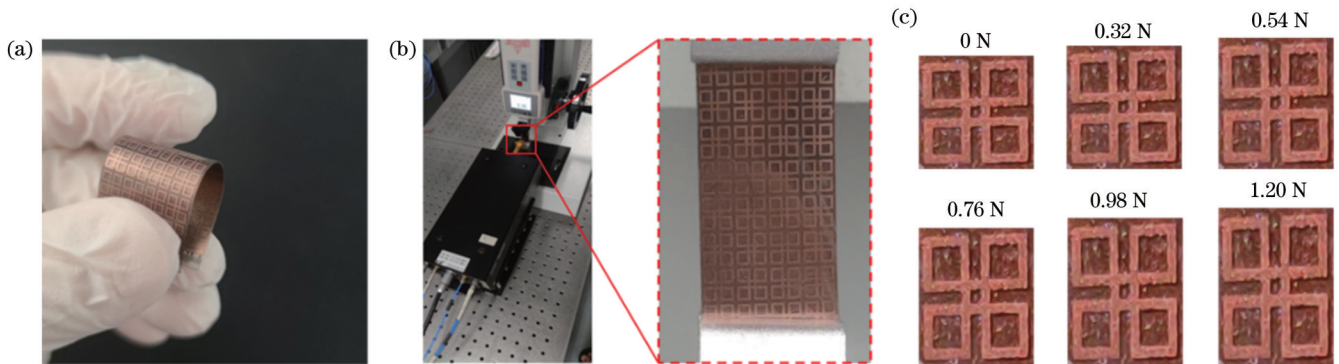


图 4 测试方案和测试结果。(a)加工得到的样品；(b)测量装置平台；(c)不同拉力下周期单元的变化情况

Fig. 4 Measurement setup and results. (a) Fabricated sample; (b) measurement setup; (c) variation of unit cell under different tension

作用在样品上的拉力和应变之间的关系可以表示为

$$E_s = \frac{F}{S\epsilon}, \quad (3)$$

式中: E_s 是弹性模量; F 是拉力; S 是样品的横截面积。考虑到拉伸率 ϵ 与拉力 F 呈线性关系, 由于 PDMS 材料的弹性模量是 2.4 MPa, 因此通过施加 1.2 N 的拉力即可将传感器的拉伸率提升为 1.2。图 4(c) 给出了不同拉力下周期单元的变化情况。图 5(a) 和 (b) 则给出了在各个拉力下模拟和测量得到的传感器的反射系数频谱。当施加在传感器上的拉力从 0 增大到 1.2 N

时, 测试得到的谐振频率从 109.23 GHz 移动到 99.42 GHz, 这与模拟结果 (从 108.88 GHz 到 99.08 GHz) 十分吻合。实验结果还表明, 不同应变下的谐振频率均具有较高的分辨率。测试得到的样品在不同拉力下的反射频谱如图 5(c) 所示, 通过线性拟合得到的传感灵敏度为 8.43 GHz/N, 测试范围为 0~1.2 N, 分辨率可达 0.06 N。根据图 5(a) 和 5(b) 的测试数据与模拟数据之间的极值误差在量程范围内的比值来定义精度^[21], 对所设计的柔性传感器的精度进行了计算分析, 精度误差能够达到 5.9%。因此该设计可以实现高精度的微小应力传感。

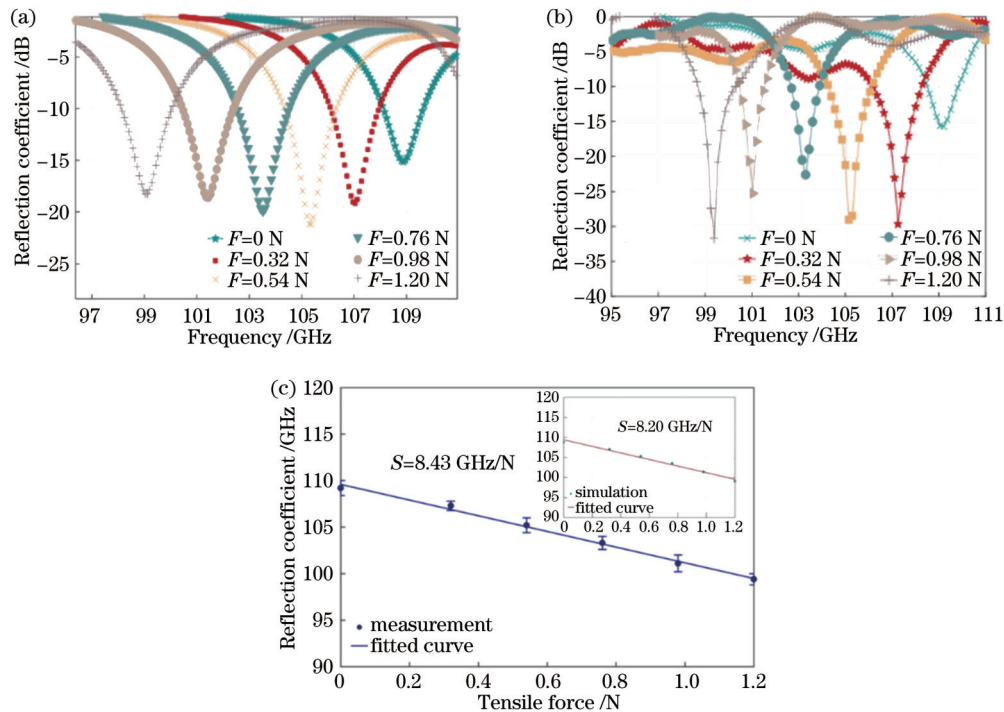


图 5 样品的传感性能表征。(a) 模拟和 (b) 测试得到的超材料传感器在不同拉力下的反射频谱; (c) 传感器的灵敏度
Fig. 5 Sensing performance of sample. (a) Simulated and (b) measured reflection spectra of metamaterial sensor under different tensile forces; (c) sensitivity of sensor

耐久性测试是一种测试器件在长时间使用下的寿命和性能差异的过程, 也是衡量传感器可靠性的重要指标。图 6 给出了样品在多次的拉伸-松弛循环后, 在初始状态 (未施加外应力) 下的电磁响应频谱。从图 6(a) 和 (b) 可以看出, 在 100 次循环之前, 谐振频率稳定在 109 GHz 左右, 随着循环数的增加谐振频率逐渐向低频区域移动。同时, 谐振的 Q 值并没有出现明显的下降。因此, 耐久性测试表明该样品至少可以经历 100 次拉伸-松弛循环。图 6(c) 表明, 随着拉伸-松弛循环次数的增加, 金属图案出现裂纹, 最终导致了结构的失效。所设计的柔性衬底超材料拉力传感器具有结构简单和成本低等特点, 在达到使用极限后, 可以直接更换传感器元件以满足传感准确性要求。

4 结 论

提出了一种基于超材料的柔性传感器, 并通过实验验证了其高灵敏度的拉力传感性能。通过拉伸该结构的柔性 PDMS 衬底, 可以改变刻蚀在衬底上的超表面的结构尺寸, 从而改变传感器的谐振频率。因此, 利用频谱分析的方法可以实现对应力和应变的传感。通过对谐振单元的优化设计, 实现了 8.43 GHz/N 的拉力传感灵敏度。所提出的传感器能够分辨出细微的拉力变化, 当施加拉力从 0 增加到 1.2 N 时, 谐振频率从 109.23 GHz 红移到 99.42 GHz。对谐振机理的研究表明, 谐振结构中央的方形连接环起到了不对称分裂间隙的作用, 激发了具有更高 Q 值的高阶谐振模式, 从而实现了更高的频谱分辨率。此外, 耐久性测试表明该样品在使用过程中至少可以经历 100 次拉伸-松弛

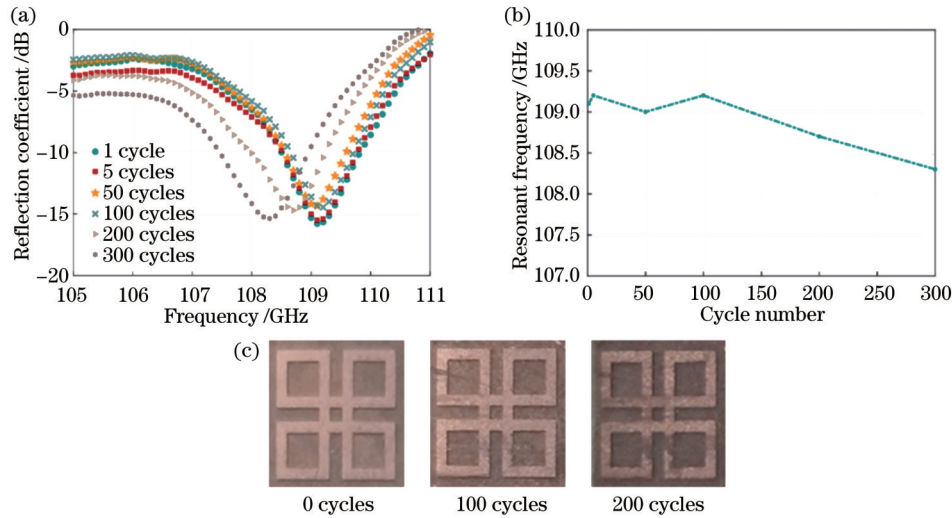


图6 不同拉伸-松弛循环次数下样品的响应特性变化。(a)反射频谱和(b)谐振频率随循环次数的变化情况;(c)不同循环次数下的单元结构照片

Fig. 6 Variation of response characteristics of sample under different stretch-relaxation cycles. Variations of (a) reflection spectrum and (b) resonant frequency with increasing number of stretch-relaxation cycle; (c) photos of unit cell structure with different stretching cycles

循环。所提出的传感器具有灵敏度高、加工方便、成本低和无线测量的优点,具有潜在的应用价值。

参 考 文 献

- [1] Ma J H, Wang P, Chen H Y, et al. Highly sensitive and large-range strain sensor with a self-compensated two-order structure for human motion detection[J]. ACS Applied Materials & Interfaces, 2019, 11(8): 8527-8536.
- [2] Li Y, Luo S D, Yang M C, et al. Poisson ratio and piezoresistive sensing: a new route to high-performance 3D flexible and stretchable sensors of multimodal sensing capability [J]. Advanced Functional Materials, 2016, 26(17): 2900-2908.
- [3] Surjadi J U, Gao L B, Du H F, et al. Mechanical metamaterials and their engineering applications[J]. Advanced Engineering Materials, 2019, 21(3): 1800864.
- [4] Hwang T Y, Choi Y, Song Y, et al. A noble gas sensor platform: linear dense assemblies of single-walled carbon nanotubes (LACNTs) in a multi-layered ceramic/metal electrode system (MLES)[J]. Journal of Materials Chemistry C, 2018, 6(5): 972-979.
- [5] Amjadi M, Kyung K U, Park I, et al. Stretchable, skin-mountable, and wearable strain sensors and their potential applications: a review[J]. Advanced Functional Materials, 2016, 26(11): 1678-1698.
- [6] Yu H, Lian Y L, Sun T, et al. Two-sided topological architecture on a monolithic flexible substrate for ultrasensitive strain sensors[J]. ACS Applied Materials & Interfaces, 2019, 11(46): 43543-43552.
- [7] Lou Z, Wang L L, Jiang K, et al. Programmable three-dimensional advanced materials based on nanostructures as building blocks for flexible sensors[J]. Nano Today, 2019, 26: 176-198.
- [8] Long Y, Zhao X L, Jiang X, et al. A porous graphene/polydimethylsiloxane composite by chemical foaming for simultaneous tensile and compressive strain sensing[J]. FlatChem, 2018, 10: 1-7.
- [9] Liu H, Li Q M, Zhang S D, et al. Electrically conductive polymer composites for smart flexible strain sensors: a critical review[J]. Journal of Materials Chemistry C, 2018, 6(45): 12121-12141.
- [10] Kim T, Cho M, Yu K. Flexible and stretchable bio-integrated electronics based on carbon nanotube and graphene[J]. Materials, 2018, 11(7): 1163.
- [11] 王庆芳, 王泽云, 韩超, 等. 基于太赫兹超材料芯片的生物混合物定量检测研究[J]. 中国激光, 2021, 48(23): 2314001. Wang Q F, Wang Z Y, Han C, et al. Quantitative detection of biological mixtures based on terahertz metamaterial chip[J]. Chinese Journal of Lasers, 2021, 48(23): 2314001.
- [12] Jing X F, Qin G H, Zhang P. Broadband silicon-based tunable metamaterial microfluidic sensor[J]. Photonics Research, 2022, 10(12): 2876-2885.
- [13] 裘燕青, 王钢棋, 郎婷婷. 基于双开口环结构的太赫兹超材料生物传感器[J]. 光学学报, 2023, 43(4): 0428002. Qiu Y Q, Wang G Q, Lang T T. Terahertz metamaterial biosensor based on double split-ring structure[J]. Acta Optica Sinica, 2023, 43(4): 0428002.
- [14] 杨洁萍, 王民昌, 邓璇, 等. 超材料吸收器集成微流控的双带太赫兹传感器[J]. 光学学报, 2021, 41(23): 2328001. Yang J P, Wang M C, Deng H, et al. Dual-band terahertz sensor based on metamaterial absorber integrated microfluidic[J]. Acta Optica Sinica, 2021, 41(23): 2328001.
- [15] Luo Z W, Hu X T, Tian X Y, et al. Structure-property relationships in graphene-based strain and pressure sensors for potential artificial intelligence applications[J]. Sensors, 2019, 19(5): 1250.
- [16] Pryce I M, Aydin K, Kelaita Y A, et al. Highly strained compliant optical metamaterials with large frequency tunability [J]. Nano Letters, 2010, 10(10): 4222-4227.
- [17] Zheng L R, Sun X Y, Xu H, et al. Strain sensitivity of electric-magnetic coupling in flexible terahertz metamaterials[J]. Plasmonics, 2015, 10(6): 1331-1335.
- [18] Li J N, Shah C M, Withayachumnankul W, et al. Mechanically tunable terahertz metamaterials[J]. Applied Physics Letters, 2013, 102(12): 121101.
- [19] Jeong H, Cui Y P, Tentzeris M M, et al. Hybrid (3D and inkjet) printed electromagnetic pressure sensor using metamaterial absorber[J]. Additive Manufacturing, 2020, 35: 101405.
- [20] Lu T G, Zhang D W, Qiu P Z, et al. Ultrathin terahertz dual-band perfect metamaterial absorber using asymmetric double-

- split rings resonator[J]. *Symmetry*, 2018, 10(7): 293.
- [21] Liang G H, Wang Y C, Mei D Q, et al. Flexible capacitive tactile sensor array with truncated pyramids as dielectric layer for three-axis force measurement[J]. *Journal of Microelectromechanical Systems*, 2015, 24(5): 1510-1519.
- [22] Lipomi D J, Vosgueritchian M, Tee B C K, et al. Skin-like pressure and strain sensors based on transparent elastic films of carbon nanotubes[J]. *Nature Nanotechnology*, 2011, 6(12): 788-792.
- [23] Amjadi M, Pichitpajongkit A, Lee S J, et al. Highly stretchable and sensitive strain sensor based on silver nanowire-elastomer nanocomposite[J]. *ACS Nano*, 2014, 8(5): 5154-5163.
- [24] Guo J J, Liu X Y, Jiang N, et al. Highly stretchable, strain sensing hydrogel optical fibers[J]. *Advanced Materials*, 2016, 28(46): 10244-10249.

Tension Sensors with High Sensitivity Based on Flexible Metamaterial

Deng Guangsheng^{1,2*}, Fang Linying², Guo Aoran², Yang Jun^{1,2}, Li Ying^{1,2}, Yin Zhiping^{1,2}

¹Special Display and Imaging Technology Innovation Center of Anhui Province, Academy of Opto-Electric Technology, Hefei University of Technology, Hefei 230009, Anhui, China;

²Anhui Province Key Laboratory of Measuring Theory and Precision Instrument, School of Instrument Science and Opto-Electronics Engineering, Hefei University of Technology, Hefei 230009, Anhui, China

Abstract

Objective Flexible electronic devices have unique ultra-thin, bendable, and lightweight features, which pave the way for developing the next generation of human motion detection, health monitoring, and wearable devices. As an important medium for collecting external mechanical signals, flexible tension sensors correspond to an indispensable component of flexible sensing systems. Given the massive potential of the sensors for applications ranging from electronic skin to real-time medical health monitoring, it is urgently needed to develop flexible, and highly stretchable and sensitive tension sensors. In this regard, achieving a high sensitivity and a large tension range simultaneously is still a bottleneck to be broken. Metamaterial has caught much attention in recent years. As an artificial structure, its electromagnetic response can be manipulated by changing the structural parameters to lay the foundation for its applications in sensing scenarios. Compared with the conventional and natural materials that have difficulty in interacting with electromagnetic waves, it overcomes this limitation, and the enhanced light-matter interaction within metamaterial can significantly improve the sensing performance. The advantages including light weight, low cost, and portability of metamaterial sensors have attracted many researchers. However, a well-designed resonant structure with a high Q factor which is also highly sensitive to structural deformation is urgently needed to further increase the sensitivity of metamaterial sensors.

Methods Firstly, a tension sensor based on electromagnetic metamaterial is designed. More specifically, the electromagnetic response of the proposed structure composed of a metallic resonator etched on the surface of polydimethylsiloxane (PDMS) can be dynamically tuned by stretching the flexible PDMS substrate. Then, deformation or tension sensing with high sensitivity can be achieved by the proposed metamaterial-based sensor. Meanwhile, we adopt a configuration containing multiple connected square patterns whose resonances are highly sensitive to the structural dimensions to improve the sensitivity. The finite element method is utilized to simulate the reflection spectrum of the model under the applications of different deformations with different tensions. Additionally, the electromagnetic response mechanism of the sensor is systematically studied by the surface current distributions. The sensor consisting of 4×10 cells is fabricated, and the extracted reflection spectra of the samples by employing different tensions are tested by applying the free space method. Furthermore, we conduct a comparison and analysis of the simulated results.

Results and Discussions We propose a tension sensor based on electromagnetic metamaterial (Fig. 1). The surface current distribution on the metallic pattern of the sensor is simulated to investigate the resonance mechanism of the proposed metamaterial. By stretching the proposed flexible metamaterial, the structural dimensions along the tension direction will be enlarged proportionally, consequently resulting in the variation of peak resonance frequency (Fig. 2). Progressively, the influence of structural parameters on sensitivity of the proposed sensor is then analyzed (Fig. 3). The flexible metamaterial sensor with 4×10 cell arrays is fabricated by performing photolithography on a 0.3 mm thick PDMS substrate, and the free space method is leveraged to measure the reflection spectra of the sensor under different tension (Fig. 4). By increasing the tension on the sensor from 0 to 1.2 N, we experimentally observe that the resonance peak frequency experiences redshift from 109.23 GHz to 99.42 GHz, which agrees well with the simulated results which have a shift from 108.88 GHz to 99.08 GHz. Meanwhile, the fitted sensitivity from the measurement results is 8.43 GHz/N,

which matches well with the sensitivity of 8.20 GHz/N in simulations (Fig. 5). Finally, the response spectra of the sample at different number of stretch-relaxation cycles are investigated, and the durability test shows that the sample repeatability can be maintained up to 100 repeated stretch-relaxation cycles (Fig. 6).

Conclusions We put forward a flexible sensor based on metamaterial, and experimentally demonstrate its applications in tension sensing with high sensitivity. By stretching the flexible PDMS substrate of the proposed structure, the structural dimension of the metasurface fabricated on the substrate can be adjusted, which allows for resonance frequency tuning. Meanwhile, we experimentally demonstrate a tension sensitivity of 8.43 GHz/N of the proposed sensor by introducing multiple square patterns with resonances highly sensitive to their structural geometry. The proposed concept is certainly capable of identifying small tension variations, which means that by increasing the tension from 0 to 1.2 N, an obvious frequency redshift from 109.23 to 99.42 GHz is observed. Additionally, the investigation of sensing mechanisms reveals that the asymmetry in the resonant structure design leads to high-order dipole resonances with higher Q value and frequency selectivity. Moreover, the durability test indicates that the sample repeatability can be maintained for at least 100 stretch-relaxation cycles. Our proposed sensor, with advantages of high sensitivity, easy fabrication, low cost, and small size, is potentially useful in deformation or tension sensing for conformal applications.

Key words sensor; tension sensor; flexibility; metamaterial; spectra; high sensitivity